3928 *Biochemistry* **2009,** *48,* 3928–3935
DOI:10.1021/bi9002106

BIOCHEMISTRY
including biophysical chemistry & molecular biology
Article

Development of Spin-Labeled Pargyline Analogues as Specific Inhibitors of Human Monoamine Oxidases A and B[†]

Anup K. Upadhyay and Dale E. Edmondson*

Departments of Biochemistry and Chemistry, Emory University, Atlanta, Georgia 30322

Received February 9, 2009. Revised Manuscript Received March 17, 2009

ABSTRACT: Three TEMPO-conjugated pargyline analogues (ParSL-1, ParSL-2, and ParSL-3) have been synthesized and their inhibitory properties tested for the two human monoamine oxidase isoforms (hMAOA and hMAOB). The three analogues differ in flexibility and substituent positions (*para* or *meta*) of the linkers connecting the TEMPO group to the pargyline phenyl ring. ParSL-1 contains a flexible acetamido (−CH_2−CO−NH−) linker connecting the two moieties at the *para* position. In contrast, the TEMPO moieties in ParSL-2 and ParSL-3 are attached with rigid amido (−CO−NH−) linkers to the *para* or *meta* positions of the pargyline phenyl ring, respectively. These variations in conformational flexibility and substituent position are shown to have profound effects in tuning the specificities of these analogues toward the two MAO isoforms. ParSL-1 irreversibly inhibits either MAOA and MAOB, ParSL-2 inhibits only MAOB (K_i = 15 ± 5 μM), and ParSL-3 is found to be specific for MAOA (K_i = 268 ± 72 μM). These results thus provide additional insights into the role of conformational flexibility and structural properties of MAO inhibitors in tuning their isoform specificities. These active site probes have been used to determine the topological orientation of these enzymes in the mitochondrial membrane. Studies with intact mitochondria show MAOA is topologically on the cytosolic face of the outer membrane in human placenta but recombinant MAOA is situated on the opposite inner face in *Pichia* mitochondria. Recombinant MAOB is found to be situated on the cytosolic face of the outer membrane in *Pichia* mitochondria.

Of the spectroscopic probes available for membrane-bound proteins, nitroxide spin labels are considered the most useful in defining structural properties of these important class of proteins. With advances in EPR[1] and NMR methodologies, the design of enzyme-specific paramagnetic spin probes will allow understanding structural properties of these proteins in their native membrane-bound forms which can be extended to tissue samples as well as to subcellular organelles. Recent studies on human and rat monoamine oxidases (MAOA and MAOB) utilized a MAO-specific pargyline analogue containing a TEMPO spin label to show differences in active site accessibility (*1*) as well as demonstrated that both isoforms are dimeric in their respective membrane-bound forms in the outer mitochondrial membrane (OMM) (*2*). The crystal structures of hMAOA (*3*, *4*) and hMAOB (*5*) exhibit overall similarities in Cα-protein folds, as expected from their high sequence identities (ca. 70%). However, the structural properties of their active site cavities are quite different. The active site of hMAOB is dipartite with a substrate binding cavity (420 Å^3) and a substrate entrance cavity (290 Å^3) (*5*) separated by Ile199, whose side chain functions as a gate in regulating substrate/inhibitor binding (*6*). In contrast, the active site in hMAOA consists of a single substrate binding cavity (550 Å^3), which appears to provide more conformational flexibility for bound ligands than the dipartite cavity in hMAOB (*3*).

An alternative approach to understand the structural properties of the active site cavities in the two human MAOs is doing structure−activity relationship (SAR) studies on the two enzymes using a series of structurally different substrate or inhibitor analogues. Such studies have been reported on human MAOA, on bovine MAOB, and on the two rat MAOs using various modified inhibitors (pargyline, clorgyline) and substrate (benzylamine) analogues (*7*−*13*). The SAR studies using a series of ring-substituted pargyline analogues on rat MAOA and MAOB (rMAOA and rMAOB) have shown that the position of substitution on the aromatic ring of pargyline (*meta* vs *para*) influences the isoform specificities of the corresponding inhibitor analogues. For example, the substitutions at the *para* position of the phenyl ring in pargyline make the corresponding analogues more specific

[†]This work was supported by NIH Grant GM-29433 to D.E.E.
*Corresponding author. Phone: 404-727-5972. Fax: 404-727-2738. E-mail: deedmon@emory.edu.
[1]Abbreviations: MAO, monoamine oxidase; ParSL, spin-labeled pargyline analogue; OGP, *n*-octyl β-D-glucopyranoside; OMM, outer mitochondrial membrane; EPR, electron paramagnetic resonance; SAR, structure−activity relationship; TEMPO, 2,2,6,6-tetramethylpiperidinyl-1-oxyl.

 Published on Web 3/18/2009

toward rMAOB, whereas the same substitutions at the *meta* positions of the ring tune the specificities of the associated analogues toward rMAOA. Based on these observations, it was concluded that the active site cavity in rMAOA has an increased lateral volume, whereas the cavity in rMAOB is more extended longitudinally. A similar study with clorgyline analogues on the two rat MAOs has shown the importance of ring substitutions and side chain structures in determining the isoform specificities of these inhibitors.

No detailed SAR study on human MAOB has been reported so far. Although the available X-ray structural data on hMAOB, showing a longer and narrower active site cavity than that in hMAOA, are consistent with the SAR studies reported on rat and bovine MAOBs, recent studies have shown that the specificities of different MAOB inhibitors are up to 2 orders of magnitude different between human and rat (*1*, *3*). Similar differences have also been reported between human and bovine MAOBs due to an Ile199Phe mutation in hMAOB, which has been shown in previous studies to prevent the binding of longer inhibitors (e.g., *trans*,*trans*-farnesol) into the bovine MAOB active site (*6*). Therefore, although previous SAR studies provided useful information on structural differences between rat MAOA and MAOB active sites in general, the extrapolation of these conclusions directly to the human enzymes is tenuous.

Development of spin-labeled and fluorescent-labeled inhibitors for use as MAOA or MAOB active site specific spectroscopic probes has been reported in previous studies (*2*, *15*, *16*). However, none of these inhibitors exhibit absolute specificity toward either specific MAO isoform. Although the nonspecific nature of these previous inhibitors makes them generally useful as MAO active site specific spectroscopic probes, their applications are limited to the recombinant enzymes in purified or membrane-bound forms or to the few biological tissues where only one enzyme isoform exists. Therefore, development of MAO spin probes with absolute isoform specificities will benefit further spectroscopic studies on these enzymes in biological tissue samples where both isoforms coexist.

In this work, using the information available from previous SAR studies and from X-ray structural data on the two human enzymes, we have designed two new pargyline-based spin-labeled inhibitors, ParSL-2 and ParSL-3 (Figure 1), which are shown to be mechanism-based, covalent inhibitors with absolute specificities toward MAOB and MAOA, respectively. The inhibitory properties of these two compounds are determined and compared with those reported earlier for the nonisoform-specific, TEMPO-substituted mechanism-based MAO inhibitor ParSL-1 (*1*). The covalent N(5)-flavocyanine adducts formed by these inhibitors with human MAOA or MAOB have been characterized by UV−vis and cw-EPR spectroscopic techniques. The structural basis for the absolute isoform specificities of ParSL-2 and ParSL-3 is discussed in the light of known X-ray crystal structures of hMAOA and hMAOB and conformational differences between the two inhibitors. Applications of these spin probes to determine the topological properties of MAOA and MAOB in intact mitochondria are demonstrated.

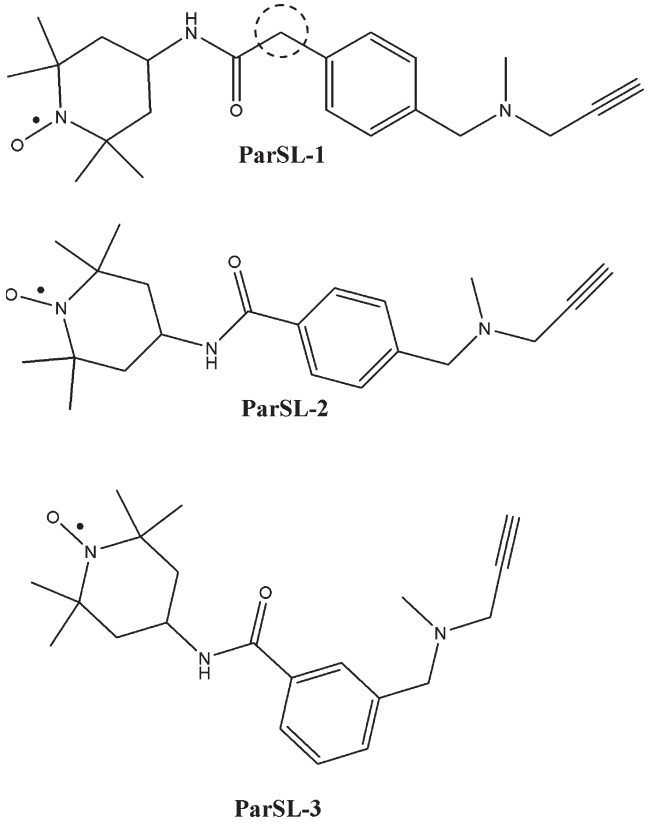

FIGURE 1: Structures of the three ParSL analogues used in this study. ParSL-1 has been reported in our previous studies (*1*, *2*) and is shown in this work for comparison. The flexible $-CH_2$ center in the ParSL-1 linker is highlighted with a dashed circle.

MATERIALS AND METHODS

Synthesis of ParSL-1 and ParSL-2. ParSL-1 was synthesized by following the method reported earlier (*1*). ParSL-2 was synthesized following a similar protocol as reported for ParSL-1, except using a different starting material. 4-(Bromomethyl)phenylacetic acid (Sigma-Aldrich) used in ParSL-1 synthesis was substituted with 4-(bromomethyl)benzoic acid (Sigma-Aldrich) for the synthesis of ParSL-2. All of the other steps and reagents involved in the synthesis were the same for both inhibitors. The crude ParSL-2 product was further purified by flash chromatography on a silica gel 60 (70−200 mesh; Merck) column using 25:75 (v/v) ethyl acetate:hexane solvent mixture. The purified product was further characterized by ESI-MS showing a m/z peak at 357.24 Da ($M + 1H^+$) in the positive ion mode.

Synthesis of ParSL-3. Approximately 800 mg (3.5 mmol) of methyl 3-(bromomethyl)benzoate (Sigma-Aldrich) was treated with 10 mL of freshly distilled ice-cold *N*-methylpropargylamine (Sigma-Aldrich). The reaction mixture was slowly warmed to room temperature and left under a N_2 atmosphere in the dark for 3 h with stirring. The reaction mixture was then evaporated to dryness under vacuum and the residue dissolved in chloroform. The chloroform solution was washed three times with distilled water and then dried with anhydrous sodium sulfate. The dried chloroform solution was then evaporated to dryness, and the intermediate methyl 3-[(methyl-2-propynylamino) methyl]benzoate (**I**) ester was further purified on a silica gel 60 column (70−200 mesh, Merck) by flash chromatography

using a 20:80 (v/v) ethyl acetate:hexane solvent mixture. Purified **I** was characterized by ESI-MS. Nearly 700 mg of the ester intermediate (**I**) was obtained at ca. 90% yield. Approximately 450 mg (~2 mmol) of **I** was dissolved in 25 mL of toluene, 10 mL of 0.2 M NaOH was added, and the mixture was refluxed for 1 h to hydrolyze the ester. The reaction mixture was acidified with a minimum volume of 5 N HCl and evaporated to dryness. The dried product mixture was extracted three times with 50 mL portions of chloroform which were combined and evaporated to dryness. The crude 3-[(methyl-2-propynylamino)methyl] benzoic acid intermediate (**II**) was further purified on a silica gel 60 column using a 20:80 (v/v) ethyl acetate:hexane solvent mixture and characterized by ESI-MS. Approximately 300 mg (1.5 mmol) of **II** in dry toluene was added to 5 mL of thionyl chloride (Sigma-Aldrich) under a N_2 atmosphere and refluxed for 1 h. The reaction mixture was evaporated to dryness, and the acid chloride thus formed was immediately reacted with 300 mg (1.75 mmol) of 4-amino-TEMPO (Sigma-Aldrich), dissolved in 25 mL of dry THF, in an salt−ice bath (−10 °C) under a stream of dry N_2 gas in the presence of 200 mg of solid K_2CO_3. The reaction mixture was slowly warmed to room temperature and left stirring overnight. The solvent was removed *in vacuo*, and the solid residue was dissolved in chloroform. The chloroform solution was washed three times with 0.1 M K_2CO_3 solution, followed by distilled water, dried with anhydrous sodium sulfate, and evaporated to dryness. Crude ParSL-3 product was further purified by flash chromatography on a silica gel 60 column (70−200 mesh; Merck) using 40:60 (v/v) an ethyl acetate:hexane solvent mixture. The purified product showed a single mass peak with an m/z of 357.24 ($M + 1H^+$) in the ESI-MS spectrum recorded in the positive ion mode.

Expression and Purification of Human MAOs. Recombinant human MAOA and MAOB were expressed in *Pichia pastoris* and purified as reported earlier (*17*, *18*). The purified enzymes were dissolved in 50 mM KP_i buffer, pH 7.2, containing 0.8% (w/v) *n*-octyl β-D-glucopyranoside (OGP) detergent micelles.

Isolation of P. pastoris Mitochondria and OMM. Intact mitochondria from *P. pastoris* cells expressing either recombinant human MAOA or MAOB were isolated by disrupting the yeast cell walls by zymolyase treatment followed by homogenization in a glass homogenizer and sequential centrifugations (*19*). The OMMs were separated by osmotic shock and mild sonication (*19*). The OMM fraction was then purified from the mitoplasts by density gradient centrifugation on a 30−55% (w/v) sucrose density gradient prepared in 10 mM Tris-HCl buffer at pH 7.4. OMMs form a separate layer near 40−45% sucrose density, while mitoplasts and unbroken mitochondria sediment to the bottom of the tube. The OMM layer was collected and diluted 3-fold with 10 mM Tris-HCl buffer, pH 7.4, and centrifuged at 35000 rpm for 1 h on a Beckman Ti-45 rotor. Pellets were resuspended in 10 mM Tris-HCl buffer at pH 7.4 containing 10% (v/v) glycerol at a protein concentration of 10 mg/mL and stored at −80 °C until used.

Isolation of Human Placental Mitochondria and OMM. Intact mitochondria from human placenta were isolated following a method reported in the literature (*20*). Briefly, placenta was collected immediately after normal delivery and washed three times with ice-cold buffer containing 230 mM manitol, 70 mM sucrose, 5 mM MOPS, 1 mM EGTA, 0.2% (w/v) BSA, 1 mM PMSF, pH 7.4 (buffer A). The tissues were then minced in a meat grinder and homogenized. The homogenate was filtered using a surgical gauge, and the filtrate was centrifuged at 1500*g* for 15 min. The supernatant was collected and centrifuged further at 4000*g* for 15 min. The supernatant was subsequently centrifuged at 12000*g* for 15 min to obtain a crude mitochondrial pellet. The pellet was resuspended in buffer A and centrifuged at 1500*g* to remove any residual erythrocytes. The final supernatant was centrifuged at 12000*g* to obtain the mitochondrial fraction. The OMMs were isolated by subjecting the intact mitochondria to osmotic shock followed by sequential centrifugation (*21*).

Optical Spectroscopic Study and Measurements of Inhibition Kinetics. Optical spectra of the oxidized and ParSL-2- or ParSL-3-inhibited detergent-purified human MAOB and MAOA samples were recorded on a Varian Cary-50 UV−visible spectrophotometer. Inhibitions constants (K_i values) in these experiments which exhibit competitive noncovalent inhibition patterns of OMM-bound human MAOA and MAOB samples by the two inhibitors were determined by measuring relative changes in K_m values for substrates (kynuramine for MAOA, benzylamine for MAOB) in presence of four different inhibitor concentrations (*1*). All MAO activity assays were performed by monitoring the rate of product formation with time using a Perkin-Elmer Lambda 2 spectrophotometer at 25 °C in 50 mM HEPES buffer adjusted to pH 7.5. For measuring MAOA activity, the rate of oxidation of kynuramine was monitored optically at 316 nm (*12*). The activity of human MAOB was followed by monitoring the rate of oxidation of benzylamine to benzaldehyde at 250 nm (*9*).

The rates of inhibition of MAO activities in intact mitochondria or in OMM preparations were determined by measuring the loss of activity over time upon incubation with ParSL analogues at room temperature. Mitochondrial pellets (intact or OMM preparations) were resuspended in their respective buffers (see above) to give 1 unit of activity/mL. One unit of activity is defined as the amount of enzyme catalyzing the formation of 1 mmol of product per minute. The concentration of the respective ParSL analogue in each hMAOA or hMAOB sample was adjusted to ca. 4-fold of their respective K_i values (60 μM ParSL-2 or ParSL-1 in the case of MAOB, 1 mM ParSL-1 or ParSL-3 for MAOA). An aliquot of 5 μL of the enzyme−inhibitor mixture was taken out at desired time points, and the residual enzyme activity was measured. All measurements were performed in duplicate, and the average values are presented in the figures.

Cw-ESR Spectroscopic Studies. The OMM-bound and detergent-purified MAO samples for cw-EPR measurements were prepared by the same procedure as reported earlier (*1*, *2*). X-band (9.4 GHz) cw-EPR spectra were recorded using a Bruker 200D instrument equipped with a Bruker ST4102/8216 TE102 cavity. Microwave frequency was measured with a HP 4256 L frequency

counter, and the temperature was regulated by using a modified Air Products cryostat and a temperature controller with a nitrogen gas flow system. All spectra were recorded at 298 K with 100 kHz field modulation frequency and 2 G modulation amplitude, unless mentioned otherwise. Samples were loaded in quartz capillaries of 1.0 mm i.d. and 2.0 mm o.d. and placed in quartz EPR sample tubes of 3 mm i.d. and 4 mm o.d.

RESULTS

Inhibitory Properties of ParSL-1, ParSL-2, and ParSL-3. The TEMPO-conjugated pargyline derivatives (ParSL-1, ParSL-2, and ParSL-3, Figure 1) used in this work function as competitive MAOA and/or MAOB inhibitors, differing in their isoform specificities and kinetic properties. The inhibition process involves a reversible first step of enzyme−inhibitor complex formation, followed by the irreversible second step of covalent N(5) flavin adduct formation at the enzyme active sites (*13*). The kinetic parameters for the inhibition of MAOA and of MAOB activities by the flexible inhibitor ParSL-1 have been reported earlier (*2*) and are reproduced in this work (Table 1) as a comparison with those determined for the other two inhibitors (ParSL-2 and ParSL-3). As reported earlier, ParSL-1 inhibits either hMAOA and hMAOB, albeit with a 10-fold higher specificity toward hMAOB than hMAOA (Table 1). Unlike ParSL-1, ParSl-2 is absolutely specific toward MAOB. Representative hyperbolic plots for the inhibition of hMAOB activity by ParSL-2 are shown in Figure 2A. Lineweaver−Burk plots (not shown) of the data show patterns typical of competitive inhibition. Figure 2B shows a plot of the K_m(obs) vs [I] used in calculating the inhibition constant (K_i) (Table 1). ParSL-2 exhibits competitive inhibition of MAOB in its OMM-bound form with a K_i value of 15 ± 5 μM, which is comparable to the value of $K_i = 22 \pm 5$ μM of ParSL-1 reported earlier (Table 1). This reversible bindng occurs prior to an irreversible, slower covalent labeling of the enzyme. After complete inhibition of catalytic activity, removal of excess inhibitor with repeated washings does not result in any recovery of hMAOB activity, demonstrating that the inhibition is irreversible.

The third inhibitor used in this study, ParSL-3, is structurally distinct from the other two analogues (ParSL-1 and ParSL-2) in that the TEMPO moiety in ParSL-3 is attached at the *meta* position of the phenyl ring in pargyline with a rigid amido (−CO−NH−) linker. This difference in the mode of conjugation results in ParSL-3 adopting a bent conformation. This structural difference of ParSL-3 relative to ParSL-1 or -2 is reflected by its difference in enzyme specificity. Unlike ParSL-1 and ParSL-2, ParSL-3 exhibits absolute specificity toward MAOA. The inhibition constant (K_i) of MAOA inhibition by ParSL-3 was determined as described above for ParSL-2 inhibition of MAOB and is comparable to that of ParSL-1 (Table 1).

The differences and similarities in K_i values of different ParSL analogues (Table 1) correlate with their rates of inhibition of OMM-bound hMAOA and hMAOB samples. For the OMM-bound hMAOA samples (Figure 3A), the rates of inhibition with a 3−4-fold molar excess of inhibitor concentration (relative to their respective K_i values) of ParSL-1 or ParSL-3 are similar (0.09 ± 0.02 min^{-1} and 0.11 ± 0.03 min^{-1}, respectively). Likewise, for the OMM-bound hMAOB samples (Figure 3B), inhibition rates with equivalent concentrations of ParSL-1 and

Table 1: Competitive Inhibition Constants and Rate Constant for Inhibition of hMAOA and hMAOB Activities by ParSL Analogues

	K_i (μM)		$k_{inhibition}$ (min^{-1})	
inhibitor	hMAOA	hMAOB	hMAOA	hMAOB
ParSL-1[a]	212 ± 28	22 ± 5	0.09 ± 0.02	0.2 ± 0.04
ParSL-2	NI	15 ± 5	NI	0.29 ± 0.07
ParSL-3	268 ± 72	NI	0.11 ± 0.03	NI

[a] These K_i values are taken from ref *1*. NI: no Inhibition.

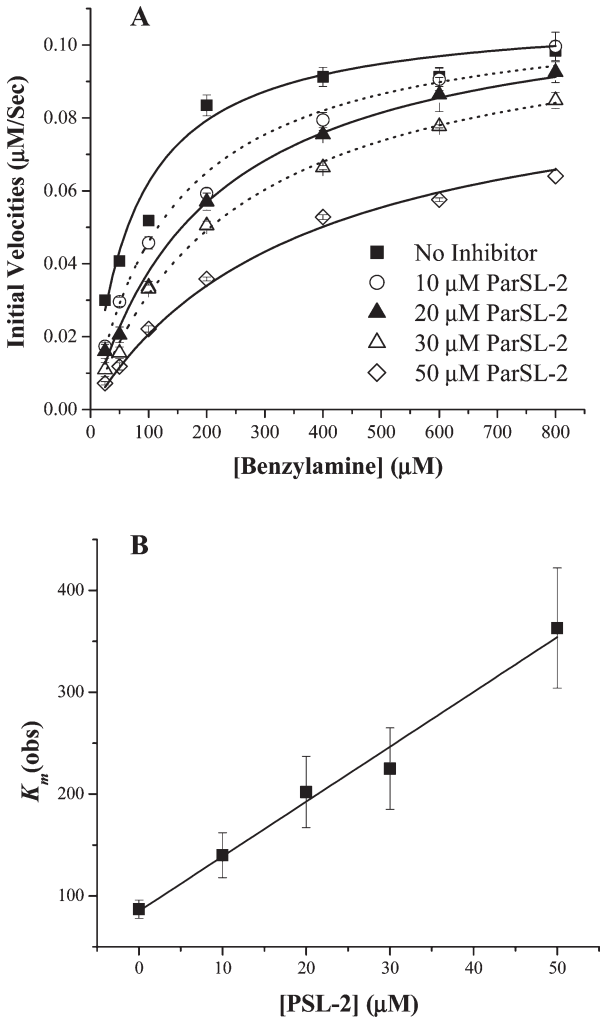

FIGURE 2: (A) A representative data set for the inhibition of hMAOB activity by various concentrations (0−50 μM) of ParSL-2 (see Figure 1) is shown. Symbols representing different ParSL-2 concentrations used are indicated. Solid lines shown are fits to the data using the Michaelis−Menten equation for a competitive-type inhibition. The fits shown are obtained by multiple regression analysis using Origin 6.0 software. The V_{max} values for all the data sets (with and without ParSL-2) were restricted to 0.1 ± 0.02 μM/s, while K_m(obs) values were floated freely. Standard deviations in K_m(obs) were calculated from the parameters obtained from three best fits. (B) Plot of apparent K_m(obs) vs inhibitor concentration ([I]) used to calculate the competitive K_i value of ParSL-2 (see Table 1).

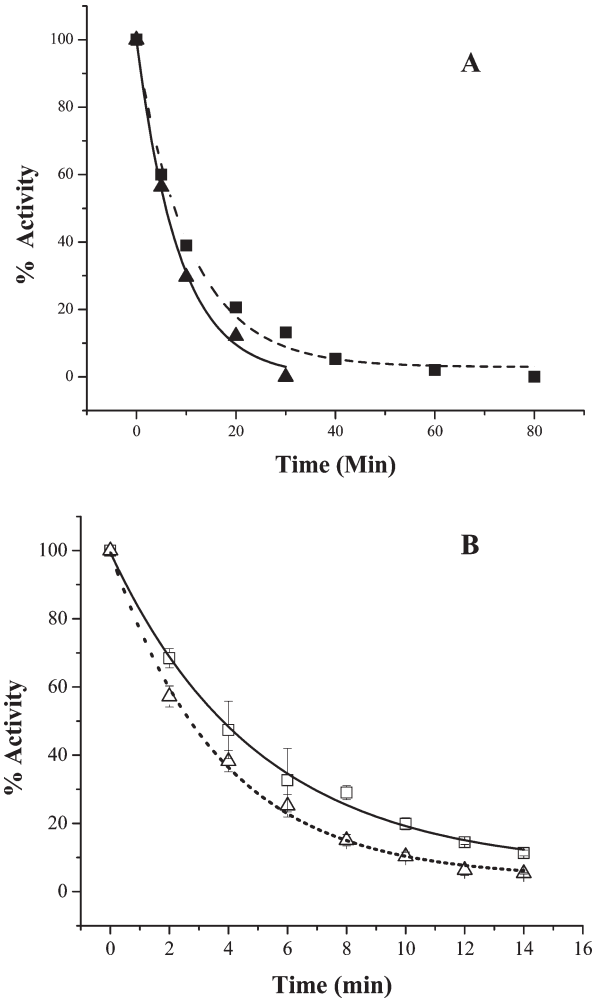

FIGURE 3: Rates of inhibition of OMM-bound (A) hMAOA with 1 mM ParSl-1 (■) and ParSL-3 (▲) and (B) hMAOB with 60 μM ParSL-1 (□) and ParSL-2 (△). The solid and dashed lines shown are exponential fits to the data generated using Origin 6.0. Apparent rate constants for inhibition are shown in Table 1.

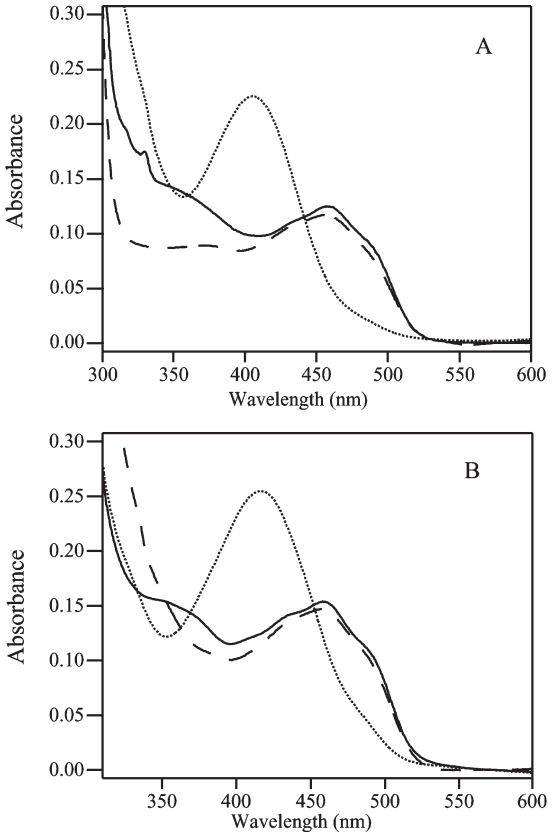

FIGURE 4: Visible absorption spectra recorded on detergent-purified hMAOB (panel A) and hMAOA (panel B) samples treated with ParSL-2 and ParSL-3 are shown. (A) hMAOB: untreated (solid line), after ParSL-2 inhibition (dotted line), and after ParSL-3 inhibition (dashed line). (B) hMAOA: untreated (solid line), after ParSL-3 inhibition (dotted line), and after ParSL-2 inhibition (dashed line).

ParSL-2 are similar (0.2 ± 0.04 min^{-1} and 0.29 ± 0.07 min^{-1}, respectively). Complete inhibition of OMM-bound hMAOB samples with either ParSL-1 or ParSL-2 requires only 10−15 min of incubation at room temperature (Figure 3B), while complete inhibition of OMM-bound hMAOA samples with ParSL-1 or ParSL-3 requires 30 min to 1 h of incubation at room temperature (Figure 3A). These differences in inhibition rates probably reflect the nearly 10-fold differences in K_i values observed between hMAOA and hMAOB (Table 1) with ParSL analogues.

Optical Spectroscopic Study. Consistent with the inhibition specificities of ParSL-2 and ParSL-3 described above, detergent-purified hMAOA and hMAOB form covalent N(5)-flavocyanine adducts only on inhibition with their respective isoform-specific pargyline analogue. The optical spectra of the untreated (solid line) and ParSL-2-inhibited (dotted line) hMAOB samples are shown in Figure 4A. The untreated sample shows an absorption peak near 456 nm due to the covalently bound flavin cofactor. On treatment with ParSL-2 a new absorption peak appears near 410 nm, demonstrating N(5)-flavocyanine adduct formation (*18*). The optical spectra recorded on the untreated (solid line) and ParSL-3-inhibited (dotted line) hMAOA samples are shown in Figure 4B. No spectral evidence for any N(5)-flavocyanine adduct formation is observed on incubation of purified hMAOB with ParSL-3 (dashed line in Figure 4A) or of hMAOA with an excess of ParSL-2 (dashed line in Figure 4B). Light scattering precludes similar absorption experiments on membrane-bound preparations of MAOA or MAOB. Previous studies in this laboratory have demonstrated that enzymes purified after inhibition by acetylenic inhibitors in their membrane-bound forms exhibit spectral properties of N(5)-flavocyanine adducts as observed with the purified, detergent-solubilized enzymes. It is most probable that the same behavior is exhibited with the TEMPO-substituted pargylines.

Cw-EPR Spectroscopic Studies. The ESR spectra recorded on ParSL-2 inhibited OMM-bound (trace A, Figure 5) and detergent-purified (trace B, Figure 5) hMAOB samples show signals characteristic of a highly immobilized protein-bound nitroxide spin label (*23*−*25*). The observed EPR signals do not decrease even after repeated washings of the samples, indicating covalent attachment of the spin probe with the protein. The OMM-bound hMAOA, treated with ParSL-2, does not show any detectable EPR signal (not shown). The EPR spectra recorded on the ParSL-3-inhibited OMM-bound and detergent-purified hMAOA samples are shown in traces C and D of Figure 5, respectively. These spectra are also consistent with a highly immobilized spin probe as

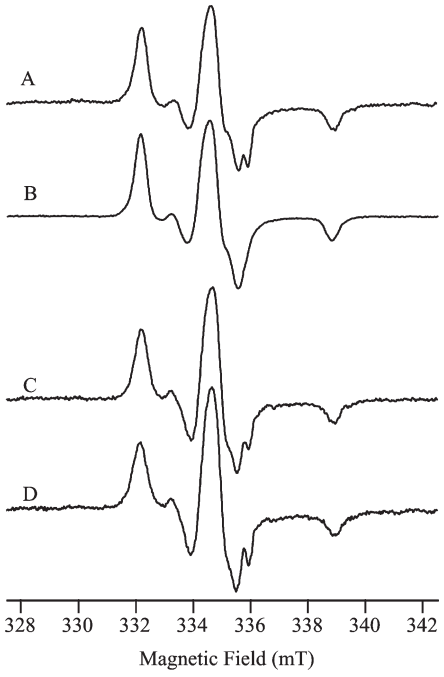

FIGURE 5: X-band EPR spectra recorded on ParSL-2- and ParSL-3-inhibited OMM-bound and purified hMAOB and hMAOA samples: (A) OMM-bound hMAOB inhibited with ParSL-2; (B) purified hMAOB inhibited with ParSL-2; (C) OMM-bound hMAOA inhibited with ParSL-3; (D) purified hMAOA inhibited with ParSL-3. All spectra are the average of 10−15 scans.

shown for MAOB. No cw-ESR signals (not shown) are observed on samples of membrane-bound MAOB incubated with ParSL-3. Control experiments performed by treating *P. pastoris* OMM not expressing either MAOA or MAOB with the ParSL analogues under similar conditions showed no significant EPR signals, demonstrating no nonspecific binding of these spin labels to the membranes at sites other than the active sites of MAOA or MAOB.

Application of ParSL-1 in Understanding Topology of MAO in Intact Mitochondria. Structural data on either MAOA or MAOB show the C-terminal domain to contain transmembrane helixes to anchor the enzymes to the outer mitochondrial membrane (*4*, *5*). The rest of the protein is then thought to fold in either the cytosolic mileu or in the space between the inner and outer mitochondrial membranes. Based on the work published by Wipf et al., it is well-known that the transport of polar nitroxide spin labels, e.g., 4-amino-TEMPO, across cellular membranes requires their attachment to a hydrophobic molecule such as a lipid side chain or a membrane-active peptide fragment (*26*). The ParSL analogues reported in this work are expected to exhibit similar membrane impermeability due to their polar nature. Therefore, activities of MAOA or MAOB in the intact mitochondria can only be inhibited by these ParSL analogues if the active sites of the two enzymes reside in the cytosolic side of the OMM.

To test the possible applicability of these ParSL analogues as probes to understand the topology of MAOA or MAOB in the mitochondrial membrane, intact mitochondria and OMMs isolated from *P. pastoris* cells, heterologously expressing either human MAOA or human MAOB, were incubated with ParSL-1, and residual MAO activities were followed as a function of time. The data in Figure 6 show that ParSL-1 rapidly inhibits MAOA activity in OMM preparations but only partially (~20%) inhibits the enzyme in intact mitochondrial preparations. In contrast, activity of the recombinant human MAOB in intact *P. pastoris* mitochondria is rapidly inhibited by ParSL-1 at a rate identical to that observed in OMM preparations. The intactness of the mitochondrial preparations was tested by comparing NADH oxidase activity using as-isolated mitochondria in isotonic buffer and sonic-disrupted mitochondria in hypotonic buffer (*27*). In both preparations, the level of NADH oxidase activity is less than 10% that of disrupted preparations showing that the mitochondrial membranes were ~90% intact. These data suggest that, in *P. pastoris* mitochondria, the active sites of the two heterologously expressed human MAOs are situated on different faces of the OMM. The active site of recombinant hMAOA situated on the inner face of the OMM, that of the recombinant hMAOB, is exposed on the cytosolic face. To determine whether similar topological behavior is also true for the naturally occurring MAOA in human, intact mitochondria (~90% intact as judged by the NADH oxidase assay) and OMM were isolated from a human placental tissue sample. This tissue is known to contain only MAOA and would therefore serve as a good comparison with the *P. pastoris* based recombinant expression system. As shown in Figure 6C, the rate of inhibition of MAOA activity by ParSL-1 is identical in both intact placental mitochondria and the corresponding OMM preparation. These results suggest that the active site of human MAOA is situated on the cytosolic face of the OMM in human placental mitochondria. Why the active sites of the two recombinant human MAOs exhibit differing topological orientation in the *P. pastoris* OMM is currently unknown and is a subject for future studies.

DISCUSSION

Results presented in this paper describe the differential inhibitory properties of two spin-labeled pargyline analogues (ParSL-2 and ParSL-3) toward MAOA and MAOB. To the best of our knowledge, the absolute specificities exhibited by these inhibitors toward MAOA or MAOB are unprecedented for any known acetylenic MAOA or MAOB inhibitors. The isoform specificities and the demonstration that they could be used for performing EPR measurements in human mitochondria make these inhibitors uniquely suitable for doing structural and functional studies on MAOs in biological materials, where they coexist (liver, brain, etc.). In addition, the molecular insights gained from these studies should provide useful information for the further development of isoform-specific acetylenic MAO inhibitors.

Structural Basis for the Enzyme Specificities of the Spin-Labeled Pargyline Analogues. The results presented show that attachment of the TEMPO moiety to the *meta* position of the phenyl ring of pargyline with a rigid amido (−CO−NH−) linker generates a MAOA-specific spin probe (ParSL-3), whereas the corresponding *para*-substituted analogue (ParSL-2) exhibits absolute specificity toward MAOB. Since the two inhibitors described

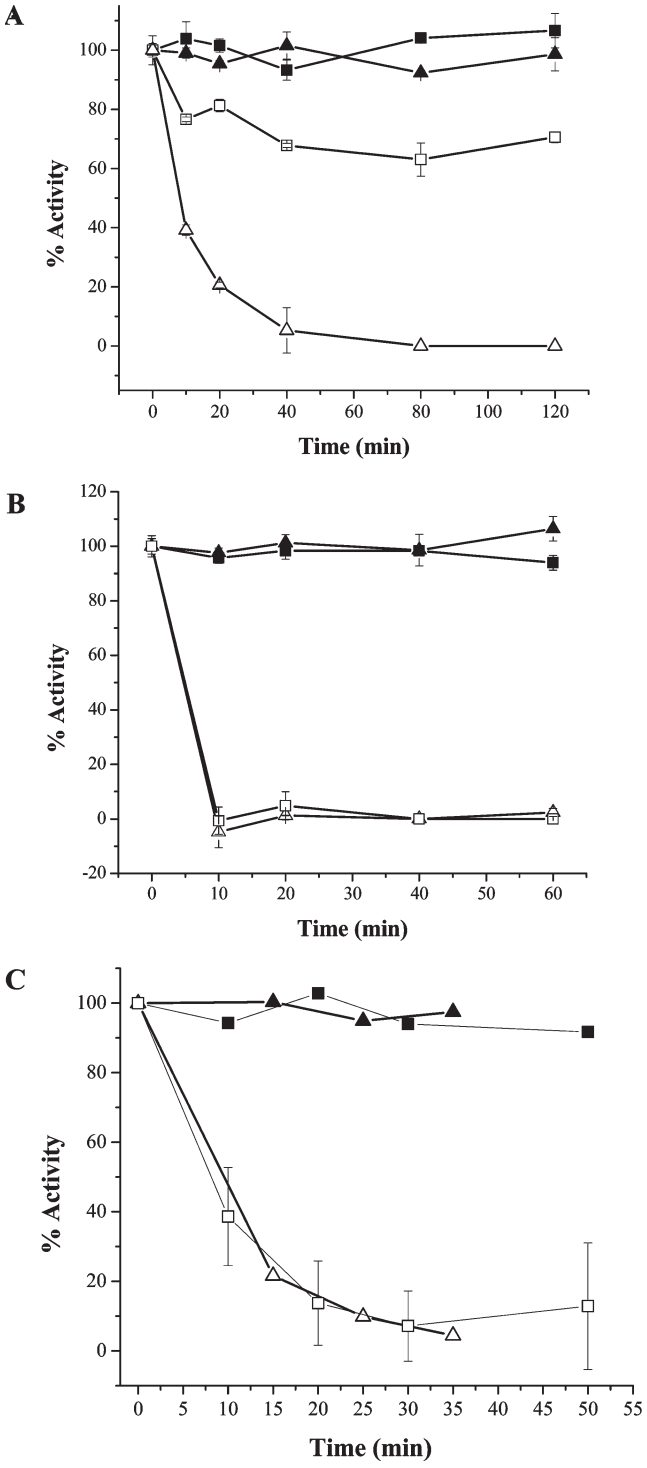

FIGURE 6: Comparison of the time dependence of MAO inhibition by ParSL-1 in intact mitochondria with enzyme in outer membrane particle preparations. In all three panels, ParSL-1 treated and untreated (control) intact mitochondrial samples are shown with empty (□) and filled (■) squares, respectively. Corresponding OMM samples are shown with empty and filled triangles (△ or ▲). (A) Inhibition time course of recombinant hMAOA in intact *P. pastoris* mitochondria and in OMM-bound forms. (B) Time course of recombinant hMAOB inhibition in intact mitochondria and in OMM preparations isolated from *P. pastoris*. (C) hMAOA inhibition in intact mitochondria and in OMM preparation isolated from human placental tissue.

above are structural isomers, with linear (ParSL-2) or bent (ParSL-3) backbone conformations of comparable flexibilities, it is obvious that the differences in their enzyme specificities originate from the structural differences in the active site cavity structures of the two MAO isoforms. It is of interest to note that *para*- and *meta*-substituted benzyloxy esters of pargyline were shown by Ali and Robinson to inhibit both rat MAOA and MAOB (*13*) although they both showed tighter binding to MAOB than to MAOA. Therefore, a possible reason that they did not observe the absolute specificity of the inhibitors examined in this study is the increased conformational flexibility of an ester linkage relative to that of an amide bond. The absolute specificity of ParSL-2 toward hMAOB is in accord with structural data which show that its active site cavity is longer with less lateral space than in hMAOA. In contrast, the absolute specificity of ParSL-3 (shorter in length with a bent conformation) toward hMAOA is consistent with the increased lateral space in the active site cavity in hMAOA compared to hMAOB. These observations are consistent with the previous QSAR studies on hMAOA and bovine MAOB (*7*−*12*).

An interesting point to note from these studies is that both of the two new spin-labeled inhibitors (ParSL-2 and ParSL-3) described in this work are derived from pargyline, which itself exhibits ca. 8-fold higher specificity toward MAOB (*22*). The X-ray structure of pargyline-inhibited hMAOB (*3*, *5*) shows that the inhibitor remains bound within the substrate binding cavity in the enzyme active site, with an empty space in the adjacent substrate entrance cavity. Examination of the available X-ray structures of hMAOB with other inhibitors of longer lengths (comparable to those of the spin-labeled inhibitors described here) shows that longer inhibitors span both cavities in hMAOB (*6*). A similar examination of the clorgyline-inhibited hMAOA crystal structure shows that clorgyline (although it can attain a linear length of comparable size as the ParSL analogues) adopts a bent conformation inside the hMAOA active site (*3*). This bent conformation of clorgyline in the hMAOA active site is possible because of its conformational flexibility, which appears to be an important component for its specificity toward MAOA. Previous SAR studies with different clorgyline analogues showed that the isoform specificities of these analogues are dependent on the length of the alkyl chain and hence to their conformational flexibilities (*8*). Therefore, shape and conformational flexibilities of these inhibitors play important roles in determining their specificities toward hMAOA or hMAOB.

Possible Applications of ParSL-2 and ParSl-3 as MAOB- and MAOA-Specific Paramagnetic Spin Probes. The demonstration of differential reactivities of human MAOA in intact mitochondria from *P. pastoris* and from human placenta using ParSL-1 (Figure 6) suggests some interesting insights may be gained from application of the isoform-specific pargyline analogues in topological studies of MAOA and MAOB in the outer mitochondrial membrane and whether this topology is altered in differing tissues. Previous experimental probes of the topology of MAOA and MAOB in the OMM used antibody reactivity (*28*) and resistance of the enzymes to protease inactivation (*29*) with inconclusive results. Additional insights into MAO topology in the membrane are important in the development and application

of MAO-specific inhibitors for use as neuroprotectants or as cardioprotectants. These compounds should be important as probes for MAO topology in rat or mice animal models used in future drug development studies. Available insights into MAO inhibitor development have shown that species differences are important in inhibitor design which should now be extended to tissue topology in different species as well. These topics constitute future aspects of MAO studies in this laboratory.

ACKNOWLEDGMENT

We thank Ms. Milagros Aldeco for providing excellent technical support. We also thank Dr. Jin Wang and Ms. Erika Milczek for helpful discussions.

REFERENCES

1. Upadhyay, A. K., Wang, J., and Edmondson, D. E. (2008) Comparison of the structural properties of the active site cavities of human and rat monoamine oxidase A and B in their soluble and membrane-bound forms. *Biochemistry 47*, 526–536.
2. Upadhyay, A. K., Borbat, P. P., Wang, J., Freed, J. H., and Edmondson, D. E. (2008) Determination of the oligomeric states of human and rat monoamine oxidases in the outer mitochondrial membrane and octyl β-D-glucopyranoside micelles using pulsed dipolar electron spin resonance spectroscopy. *Biochemistry 47*, 1554–1566.
3. De Colibus, L., Li, M., Binda, C., Lustig, A., Edmondson, D. E., and Mattevi, A. (2005) Three-dimensional structure of human monoamine oxidase A (MAO A): Relation to the structures of rat MAO A and human MAO B. *Proc. Natl. Acad. Sci. U.S.A. 102*, 12684–12689.
4. Son, S.-Y., Mat, J., Kondou, Y., Yoshimura, M., Yamashita, E., and Tsukihara, T. (2008) Structure of human monoamine oxidase A at 2.2-Å resolution: The control of opening the entry for substrates/inhibitors. *Pror. Natl. Acad. Sci. U.S.A. 105*, 5739–5744.
5. Binda, C., Newton-Vinson, P., Hubalek, F., Edmondson, D. E., and Mattevi, A. (2002) Structure of human monoamine oxidase B, a drug target for the treatment of neurological disorders. *Nat. Struct. Biol. 9*, 22–26.
6. Hubalek, F., Binda, C., Khalil, A., Li, M., Mattevi, A., Castagnoli, N., and Edmondson, D. E. (2005) Demonstration of isoleucine 199 as a structural determinant for the selective inhibition of human monoamine oxidase b by specific reversible inhibitors. *J. Biol. Chem. 280*, 15761–15766.
7. Wang, Y. X., and Castagnoli, N.Jr. (1995) Studies on the monoamine oxidase (MAO)-catalyzed oxidation of phenyl-substituted 1-methyl-4-phenoxy-1,2,3,6-tetrahydropyridine derivatives: factors contributing to MAO-A and MAO-B selectivity. *J. Med. Chem. 38*, 1904–1910.
8. O'Brien, E. M., Tipton, K. F., Meroni, M., and Dostert, P. (1994) Inhibition of monoamine oxidase by clorgyline analogues. *J. Neural. Transm., Suppl. 41*, 295–305.
9. Walker, M. C., and Edmondson, D. E. (1994) Structure-activity relationships in the oxidation of benzylamine analogues by bovine liver mitochondrial monoamine oxidase B. *Biochemistry 33*, 7088–7098.
10. Edmondson, D. E. (1995) Structure activity studies of the substrate binding site in monoamine oxidase B. *Biochimie 77*, 643–650.
11. Yu, P. H., Davis, B. A., and Boulton, A. A. (1993) Effect of structural modification of alkyl N-propargylamines on the selective inhibition of monoamine oxidase B activity. *Biochem. Pharmacol. 46*, 753–757.
12. Miller, J. R., and Edmondson, D. E. (1999) Structure-activity relationships in the oxidation of para-substituted benzylamine analogues by recombinant human liver monoamine oxidase A. *Biochemistry 38*, 13670–13683.
13. Ali, A., and Robinson, J. B. (1991) Synthesis, biological evaluation and quantitative structure activity relationship analysis of nuclear-substituted pargylines as competitive inhibitors of MAO-A and MAO-B. *J. Pharm. Pharmacol. 43*, 750–757.
14. Novaroli, L., Daina, A., Favre, E., Bravo, J., Carotti, A., Leonetti, F., Catto, M., Carrupt, P.-A., and Reist, M. (2006) Impact of species-dependent differences on screening, design, and development of MAO B inhibitors. *J. Med. Chem. 49*, 6264–6272.
15. Buckman, T., and Eiduson, S. (1980) Studies of pargyline-monoamine oxidase binding using a spin label probe analog. *J. Neurochem. 34*, 1594–1602.
16. Rando, R. R. (1977) The fluorescent labeling of mitochondrial monoamine oxidase. *Mol. Pharmacol. 13*, 726–734.
17. Newton-Vinson, P., Hubalek, F., and Edmondson, D. E. (2000) High-level expression of human liver monoamine oxidase B in *Pichia pastoris*. *Protein Expression Purif. 20*, 334–345.
18. Li, M., Hubalek, F., Newton-Vinson, P., and Edmondson, D. E. (2002) High-level expression of human liver monoamine oxidase A in *Pichia pastoris*: comparison with the enzyme expressed in *Saccharomyces cerevisiae*. *Protein Expression Purif. 24*, 152–162.
19. Daum, G., Boehni, P. C., and Schatz, G. (1982) Import of proteins into mitochondria. Cytochrome b_2 and cytochrome *c* peroxidase are located in the intermembrane space of yeast mitochondria. *J. Biol. Chem. 257*, 13028–13033.
20. Martinez, F., Kiriakidou, M., and Strauss, J. F.III (1997) Structural and functional changes in mitochondria associated with trophoblast differentiation: methods to isolate enriched preparations of syncytiotrophoblast mitochondria. *Endocrinology 138*, 2172–2183.
21. Uribe, A., Strauss, J. F.III, and Martinez, F. (2003) Contact sites from human placental mitochondria: Characterization and role in progesterone synthesis. *Arch. Biochem. Biophys. 413*, 172–181.
22. Fowler, C. J., Mantle, T. J., and Tipton, K. F. (1982) The nature of the inhibition of rat liver monoamine oxidase types A and B by the acetylenic inhibitors clorgyline, l-deprenyl and pargyline. *Biochem. Pharmacol. 31*, 3555–3561.
23. Columbus, L., and Hubbell, W. L. (2004) Mapping backbone dynamics in solution with site-directed spin labeling: GCN4-58 bZip free and bound to DNA. *Biochemistry 43*, 7273–7287.
24. Liang, Z., Lou, Y., Freed, J. H., Columbus, L., and Hubbell, W. L. (2004) A multifrequency electron spin resonance study of T4 lysozyme dynamics using the slowly relaxing local structure model. *J. Phys. Chem. B 108*, 17649–17659.
25. Barnes, J. P., Liang, Z., McHaourab, H. S., Freed, J. H., and Hubbell, W. L. (1999) A multifrequency electron spin resonance study of T4 lysozyme dynamics. *Biophys. J. 76*, 3298–3306.
26. Wipf, P., Xiao, J, Jiang, J., Belikova, N. A., Tyurin, V. A., Fink, M. P., and Kagan, V. E. (2005) Mitochondrial targeting of selective electron scavengers: Synthesis and biological analysis of hemigramicidin-TEMPO conjugates. *J. Am. Chem. Soc. 127*, 12460–12461.
27. Matsumoto, J., Sakamoto, K., Shinyo, N., Kido, Y., Yamamoto, N., Yagi, K., Miyoshi, H., Nonaka, N., Katakura, K., Kita, K., and Oku, Y. (2008) Anerobic NADH-fumarate reductase is predominant in the respiratory chain of *Echinococcus multilocaris*, providing a novel target for the chemotherapy of alveolar Echinococcosis. *Antimicrob. Agents Chemother. 52*, 164–170.
28. Russell, S. M., Davey, J., and Mayer, R. J. (1979) The vectorial orientation of human monoamine oxidase in the outer mitochondrial membrane. *Biochem. J. 181*, 7–14.
29. Buckman, T., Sutphin, M. S., and Eidusin, S. (1984) Proteases as probes of mitochondrial monoamine topography *in situ*. *Mol. Pharmacol. 25*, 165–170.